

A low harmonic 12-pulse rectifier based on zigzag autotransformer by current injection at DC side

LIU Jiongde¹, CHEN Xiaoqiang^{1,2}, WANG Ying¹, CHEN Tao¹

(1. School of Automation and Electrical Engineering, Lanzhou Jiaotong University, Lanzhou 730070, China;
2. Key Laboratory of Opto-Electronic Technology and Intelligent Control, Ministry of Education, Lanzhou Jiaotong University, Lanzhou 730070, China)

Abstract: To improve the harmonic suppression ability of multi-pulse rectifier, a 12-pulse rectifier based on zigzag autotransformer by DC side active compensation strategy is proposed. By controlling the small capacity current inverter to generate compensating currents and injecting the currents directly into the DC side of the system, the grid-side currents of the rectifier can be approximated to sine wave. Using zigzag autotransformer as phase-shifting transformer can block the zero sequence current components and reduce the equivalent capacity of the rectifying system. The study on harmonic distortion rate of grid-side currents with the variation of the load shows that the harmonic content of the compensated rectifier decreases significantly under various load conditions. The harmonic content of the grid-side currents of the proposed active injection rectifier is only 1.17%, and the equivalent capacity of the rectifier is calculated. The results show that the rectifier can not only suppress the harmonic currents, but also have a lower equivalent capacity.

Key words: multi-pulse rectifier; active compensation; zigzag autotransformer; equivalent capacity

0 Introduction

In recent years, multi-pulse rectifier technology has been widely used in high-power rectifier^[1]. Among many multi-pulse rectifiers, the 12-pulse rectifier is the most widely used, which can eliminate the 5th and 7th harmonics. The total harmonic distortion (THD) value of the grid-side current is about 15%^[2], but it cannot meet the harmonic requirements when the high-power rectifier is connected to the power grid.

Increasing the number of pulses^[3] or installing active or passive circuits on the DC or AC sides of the rectifying system can reduce the harmonic content of the grid-side currents^[4]. However, simply increasing the number of pulses will increase the difficulty of winding design and debase the accuracy of equipment manufacturing, which leads to the deterioration of system symmetry. The passive harmonic suppression method on the DC side can only suppress the lower harmonics of the grid-side currents, but helpless to

the higher harmonics suppression and will double the amplitude of the higher harmonics^[5].

An active auxiliary circuit is installed on the DC side of the 12-pulse rectifier, which can effectively eliminate $(12k_0 \pm 1)$ th harmonics as k_0 is any positive integer and make the distorted grid-side current into standard sine wave approximately^[6-8]. In Ref. [9], an active harmonic suppression method is adopted on the DC side to reduce the number of switching devices and make the structure more compact. When the matching condition of the system is satisfied, the harmonics can be suppressed effectively. A current forming method for 12-pulse rectifier is proposed in Ref. [10], in which the rectifier has a inter-phase reactor (IPR) on the AC side and two single-phase boost switch converters in parallel on the DC side. By adding boost harmonic suppression circuits on the DC side of the multi-pulse rectifier, the δ_{THD} , which represents the currents of THD rate, on the grid-side can be reduced to 1.44% and the power factor of the circuit can be improved^[11]. A compensation strategy

Received date: 2020-03-28

Foundation items: National Natural Science Foundation of China (No. 51767013); Science and Technology Research and Development Plan of China Railway Corporation (No. 2017J012-A); Lanzhou City Science and Technology Program for Innovation and Entrepreneurship of Talents (No. 2017-RC-51)

Corresponding author: LIU Jiongde (xliujdx@163.com)

based on isolated transformer multi-pulse rectifier is proposed in Refs. [12] and [13]. Compared with the deployment of multiple active power filters on AC side in Ref. [13], the control strategy of three-phase inverter used in Ref. [12] is relatively simple. A high-power rectifier based on star phase-shifting autotransformer is proposed in Ref. [14], which uses an active IPR to eliminate the harmonic of the grid-side current, and requires three IPRs with secondary windings and a current-controlled inverter.

Zigzag transformer can not only be used as grounding transformer in high voltage system^[15], but also be used as phase-shifting transformer in multi-pulse rectifying system with the advantages of simple structure and small equivalent capacity^[16]. Due to the unique characteristic of the zigzag phase-shifting transformer, it can block zero-sequence currents inside the transformer, so the zero sequence blocking transformer (ZSBT) can be omitted in the rectifier based on zigzag autotransformer^[17], thus the equivalent capacity of the system is reduced further.

In our work, a zigzag 12-pulse rectifier using active injection method on the DC side is studied. The equivalent capacity of the rectifier can be reduced by using zigzag autotransformer as a phase-shifting transformer. The injected current is realized by a single-phase inverter whose equivalent capacity is only 2.2% of the rated output power, which can effectively reduce the δ_{THD} of the grid-side and the equivalent capacity of the system without changing the system parts of original 12-pulse rectifier.

1 Structure of multi-pulse rectifier

Fig. 1 shows the schematic diagram of the zigzag 12-pulse rectifier with current injection at DC Side. The proposed rectifier consists of the three-phase voltage sources, a zigzag phase-shifting autotransformer, two groups of diode bridge rectifier (DBR) I and DBR II, the IPRs and a single-phase inverter.

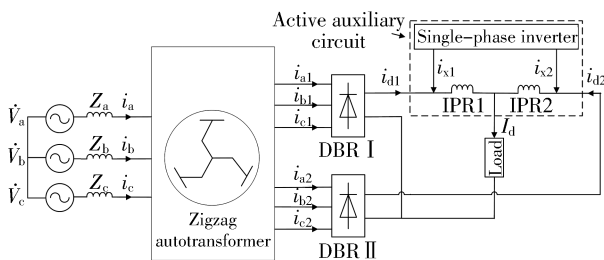


Fig. 1 Main circuit of zigzag 12-pulse rectifier with current injection at DC Side

The IPRs can absorb the instantaneous voltage difference between the two groups of DBRs, so that the two groups of DBRs can work independently. In addition, in Fig. 1, Z_a , Z_b and Z_c represent the source impedances; i_a , i_b , and i_c represent the grid-side currents, the currents i_{a1} , i_{b1} , i_{c1} and i_{a2} , i_{b2} , i_{c2} are the three-phase input currents of the DBR I and DBR II, respectively. The rectifier uses the current hysteresis-band to control the inverter to output a specific current waveform, so that the input current on the grid side is close to the sine wave. In Fig. 1, i_{x1} and i_{x2} are the specific currents generated by the single-phase inverter in the active auxiliary circuit.

2 Winding design of zigzag autotransformer

In order to make the wave number of the output current waveform be 12, the windings of the zigzag phase-shifting transformer need to be designed. Fig. 2 shows the voltage phasor-diagram of the 12-pulse zigzag autotransformer. \dot{V}_a , \dot{V}_b , \dot{V}_c are input phase voltages of the transformer, \dot{V}_{a1} , \dot{V}_{b1} , \dot{V}_{c1} and \dot{V}_{a2} , \dot{V}_{b2} , \dot{V}_{c2} are output phase voltages of the transformer. The 2α is the phase-shifting angle of output voltages of the transformer.

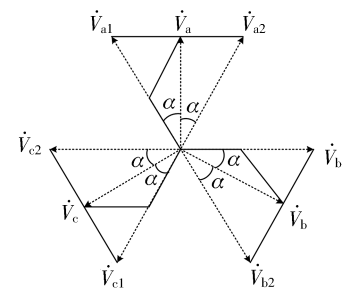


Fig. 2 Voltage phasor-diagram

The input phase voltages of the rectifier are given as

$$\begin{cases} \dot{V}_a = V_s \angle 0^\circ, \\ \dot{V}_b = V_s \angle -120^\circ, \\ \dot{V}_c = V_s \angle 120^\circ, \end{cases} \quad (1)$$

where V_s is the root-mean-square (RMS) value of phase voltages.

Therefore, the input line voltages are

$$\begin{cases} \dot{V}_{ab} = \sqrt{3}V_s \angle 30^\circ, \\ \dot{V}_{bc} = \sqrt{3}V_s \angle -90^\circ, \\ \dot{V}_{ca} = \sqrt{3}V_s \angle 150^\circ. \end{cases} \quad (2)$$

The phase-shifting transformer of the 12-pulse rectifier shall provide two sets of voltages with a phase difference of 30° ^[3], so α is 15° and here come the formulas

$$\begin{cases} \dot{V}_{a1} = V \angle 15^\circ, \\ \dot{V}_{b1} = V \angle -105^\circ, \\ \dot{V}_{c1} = V \angle 135^\circ, \end{cases} \quad (3)$$

$$\begin{cases} \dot{V}_{a2} = V \angle -15^\circ, \\ \dot{V}_{b2} = V \angle -135^\circ, \\ \dot{V}_{c2} = V \angle 105^\circ, \end{cases} \quad (4)$$

where V is the RMS value of output phase voltages of the phase-shifting transformer.

The transformation ratio K_1 and K_2 of phase-shifting autotransformer are set in Fig. 3. By Fig. 2, we can get

$$V_s = V \cos \alpha, \quad (5)$$

$$\dot{V}_{a1} = K_1(\dot{V}_{ab} - \dot{V}_{ca}) - K_2 \dot{V}_{bc}, \quad (6)$$

$$\dot{V}_{a2} = K_1(\dot{V}_{ab} - \dot{V}_{ca}) + K_2 \dot{V}_{bc}. \quad (7)$$

According to Eqs. (1)–(7), we can obtain that $K_1=0.3333$ and $K_2=0.1547$.

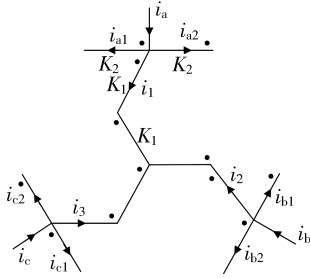


Fig. 3 Zigzag autotransformer winding configuration

3 Theory of active injection

Fig. 3 shows the winding configuration of zigzag autotransformer. In Fig. 3, currents i_1 , i_2 and i_3 represent the currents in the windings of the phase-shifting transformer. By applying Kirchhoff's Current Law, currents i_a , i_b and i_c can be expressed as

$$\begin{cases} i_a = i_{a1} + i_{a2} + i_1, \\ i_b = i_{b1} + i_{b2} + i_2, \\ i_c = i_{c1} + i_{c2} + i_3, \\ i_1 + i_2 + i_3 = 0. \end{cases} \quad (8)$$

The balance relationship of magneto motive force (MMF) of zigzag autotransformer is

$$\begin{cases} K_1 i_2 - K_1 i_3 + K_2 i_{a1} - K_2 i_{a2} = 0, \\ K_1 i_1 - K_1 i_3 + K_2 i_{b1} - K_2 i_{b2} = 0, \\ K_1 i_1 - K_1 i_2 + K_2 i_{c1} - K_2 i_{c2} = 0. \end{cases} \quad (9)$$

By Eqs. (8) and (9), the relationship between the grid-side currents i_a , i_b , i_c and the output currents i_{a1} , i_{b1} , i_{c1} , i_{a2} , i_{b2} , i_{c2} of autotransformer can be calculated as

$$\begin{cases} i_a = i_{a1} + i_{a2} + \frac{K_2(i_{c2} - i_{c1} + i_{b1} - i_{b2})}{3K_1}, \\ i_b = i_{b1} + i_{b2} + \frac{K_2(i_{a2} - i_{a1} + i_{c1} - i_{c2})}{3K_1}, \\ i_c = i_{c1} + i_{c2} + \frac{K_2(i_{b2} - i_{b1} + i_{a1} - i_{a2})}{3K_1}. \end{cases} \quad (10)$$

The relationship between the input and output sides of the DBRs can be expressed by introducing the switch function. Therefore, the grid-side currents can be presented by the mapping function and the output currents of the DBRs.

$$\begin{cases} S_{a1}(t) = 0.5 \{ \text{sign}[u_{a1}(t) - u_{c1}(t)] - \text{sign}[u_{b1}(t) - u_{a1}(t)] \}, \\ S_{b1}(t) = 0.5 \{ \text{sign}[u_{b1}(t) - u_{a1}(t)] - \text{sign}[u_{c1}(t) - u_{b1}(t)] \}, \\ S_{c1}(t) = 0.5 \{ \text{sign}[u_{c1}(t) - u_{b1}(t)] - \text{sign}[u_{a1}(t) - u_{c1}(t)] \}, \\ S_{a2}(t) = 0.5 \{ \text{sign}[u_{a2}(t) - u_{c2}(t)] - \text{sign}[u_{b2}(t) - u_{a2}(t)] \}, \\ S_{b2}(t) = 0.5 \{ \text{sign}[u_{b2}(t) - u_{a2}(t)] - \text{sign}[u_{c2}(t) - u_{b2}(t)] \}, \\ S_{c2}(t) = 0.5 \{ \text{sign}[u_{c2}(t) - u_{b2}(t)] - \text{sign}[u_{a2}(t) - u_{c2}(t)] \}, \end{cases} \quad (11)$$

where $S_{a1}(t)$, $S_{b1}(t)$, $S_{c1}(t)$, $S_{a2}(t)$, $S_{b2}(t)$, $S_{c2}(t)$ are the mapping functions of phase a_1 , phase a_2 , phase b_1 , phase b_2 , phase c_1 , phase c_2 .

The input currents of the DBRs can be expressed as

$$\begin{bmatrix} i_{a1} \\ i_{b1} \\ i_{c1} \end{bmatrix} = \begin{bmatrix} S_{a1} \\ S_{b1} \\ S_{c1} \end{bmatrix} i_{d1}, \quad (12)$$

$$\begin{bmatrix} i_{a2} \\ i_{b2} \\ i_{c2} \end{bmatrix} = \begin{bmatrix} S_{a2} \\ S_{b2} \\ S_{c2} \end{bmatrix} i_{d2}. \quad (13)$$

Meanwhile, by applying Kirchhoff's Current Law in Fig. 1, output currents of DBRs can be expressed as

$$\begin{bmatrix} i_{d1} \\ i_{d2} \end{bmatrix} = \begin{bmatrix} \frac{I_d}{2} - i_{x1} \\ \frac{I_d}{2} - i_{x2} \end{bmatrix}. \quad (14)$$

Combining Eqs. (12), (13) and (14), we can get

$$\begin{bmatrix} i_{a1} \\ i_{b1} \\ i_{c1} \\ i_{a2} \\ i_{b2} \\ i_{c2} \end{bmatrix} = \begin{bmatrix} S_{a1} \left(\frac{I_d}{2} - i_{x1} \right) \\ S_{b1} \left(\frac{I_d}{2} - i_{x1} \right) \\ S_{c1} \left(\frac{I_d}{2} - i_{x1} \right) \\ S_{a2} \left(\frac{I_d}{2} - i_{x2} \right) \\ S_{b2} \left(\frac{I_d}{2} - i_{x2} \right) \\ S_{c2} \left(\frac{I_d}{2} - i_{x2} \right) \end{bmatrix}. \quad (15)$$

By substituting Eq. (15) into Eq. (10), the grid-side currents expressed by DC load current I_d and injected compensating currents i_{x1} , i_{x2} can be written as

$$\begin{cases} i_a = (A+B) \frac{I_d}{2} - Ai_{x1} - Bi_{x2}, \\ i_b = (C+D) \frac{I_d}{2} - Ci_{x1} - Di_{x2}, \\ i_c = (E+F) \frac{I_d}{2} - Ei_{x1} - Fi_{x2}, \end{cases} \quad (16)$$

where

$$A = S_{a1} + \frac{K_2}{3K_1} (S_{b1} - S_{c1}),$$

$$B = S_{a2} + \frac{K_2}{3K_1} (S_{c2} - S_{b2}),$$

$$C = S_{b1} + \frac{K_2}{3K_1} (S_{c1} - S_{a1}),$$

$$D = S_{b2} + \frac{K_2}{3K_1} (S_{a2} - S_{c2}),$$

$$E = S_{c1} + \frac{K_2}{3K_1} (S_{a1} - S_{b1}),$$

$$F = S_{c2} + \frac{K_2}{3K_1} (S_{b2} - S_{a2}).$$

In order to ensure the full compensation of the rectifying system, the three-phase grid-side currents are set as

$$\begin{cases} i_a = \frac{2\sqrt{3}}{\pi} I_d \sin(\omega t), \\ i_b = \frac{2\sqrt{3}}{\pi} I_d \sin(\omega t - \frac{2\pi}{3}), \\ i_c = \frac{2\sqrt{3}}{\pi} I_d \sin(\omega t + \frac{2\pi}{3}). \end{cases} \quad (17)$$

From Eqs. (16) and (17), the compensating currents i_{x1} , i_{x2} can be expressed as

$$i_{x1} = \frac{\frac{2\sqrt{3}}{\pi} I_d [D \sin \omega t - B \sin(\omega t - \frac{2\pi}{3})]}{BC - AD} + \frac{1}{2} I_d, \quad (18)$$

$$i_{x2} = \frac{\frac{2\sqrt{3}}{\pi} I_d [A \sin(\omega t - \frac{2\pi}{3}) - C \sin(\omega t)]}{BC - AD} + \frac{1}{2} I_d. \quad (19)$$

The expression of compensating current i_{x1} is complex and not easy to implement in practice. Therefore, calculating Eqs. (18) by Matlab, we can

approximately obtain the waveform of the ratio of compensating current i_{x1} to DC side load current I_d , as shown in Fig. 4. The waveform of compensating current i_{x2} is the same as that of i_{x1} , but the phase difference is 30° . Under the condition of power frequency, the waveform shown in Fig. 4 can be injected into the DC side of the rectifying system to make the currents on the grid side closer to the sine wave.

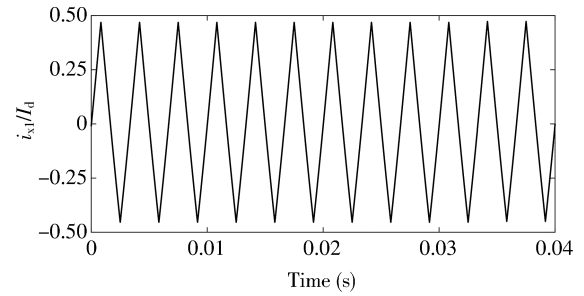


Fig. 4 Theoretical compensating waveform of i_{x1}/I_d

4 Construction of active auxiliary circuit

The single-phase inverter and the IPRs in Fig. 5 constitute an active auxiliary circuit. Combining this kind of auxiliary circuit with zigzag phase-shifting 12-pulse rectifier can not only reduce the manufacturing difficulty and winding configuration of phase-shifting transformer, but also reduce the harmonic content of rectifying system observably.

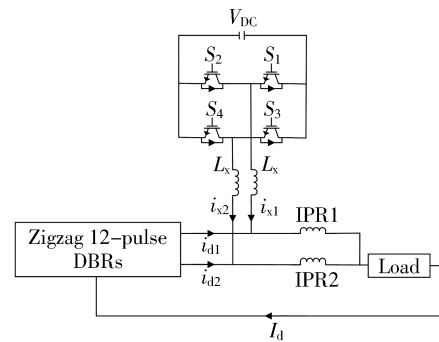


Fig. 5 Active auxiliary circuit

In Fig. 5, the output ends of the rectifier are connected to two dotted terminals of the IPRs. Similarly, as for compensating current i_{x1} and i_{x2} , the single-phase inverter generates them and feed them into the IPRs. In Fig. 5, L_x represents the filter inductance of the inverter, V_{DC} represents the DC input voltage of the inverter, and I_d represents the load current of the rectifying system. To generate the injection current waveform as shown in Fig. 4, we can replace this waveform by a standard triangular wave

as shown in Fig. 6 with a frequency of 300 Hz, that is, a period T_0 of 1/300 s and an amplitude of $0.45I_d$.

The expressions of injected compensation currents in Fig. 6 are given by

$$i_{x1}(t) = \begin{cases} \left(-\frac{1.8}{T_0} - 0.9\right)I_d, & \left(-\frac{T_0}{2} \pm kT_0, -\frac{T_0}{4} \pm kT_0\right), \\ \frac{1.8}{T_0}I_d t, & \left(-\frac{T_0}{4} \pm kT_0, \frac{T_0}{4} \pm kT_0\right), \\ \left(-\frac{1.8}{T_0}t + 0.9\right)I_d, & \left(\frac{T_0}{4} \pm kT_0, \frac{T_0}{2} \pm kT_0\right), \end{cases} \quad (k = 0, 1, 2, \dots), \quad (20)$$

$$i_{x2}(t) = \begin{cases} \left(-\frac{1.8}{T_0} - 0.9\right)I_d, & \left(\pm kT_0, \frac{T_0}{4} \pm kT_0\right), \\ \frac{1.8}{T_0}I_d t, & \left(\frac{T_0}{4} \pm kT_0, \frac{3T_0}{4} \pm kT_0\right), \\ \left(-\frac{1.8}{T_0}t + 0.9\right)I_d, & \left(\frac{3T_0}{4} \pm kT_0, T_0 \pm kT_0\right). \end{cases} \quad (k = 0, 1, 2, \dots). \quad (21)$$

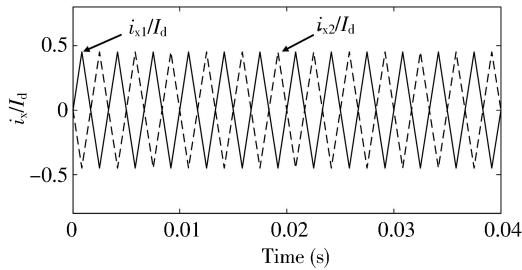


Fig. 6 Injected triangular waveforms

The Fourier series expansions of Eqs. (20) and (21) are

$$\begin{cases} i_{x1} = \frac{8AI_d}{\pi^2} \sum_{n=1,3,5,\dots}^{\infty} \frac{(-1)^{\frac{n-1}{2}}}{n^2} \sin(n\omega t), \\ i_{x2} = -\frac{8AI_d}{\pi^2} \sum_{n=1,3,5,\dots}^{\infty} \frac{(-1)^{\frac{n-1}{2}}}{n^2} \sin(n\omega t), \end{cases} \quad (22)$$

where T_0 is 1/300, A is the amplitude of the 6 times the power frequency triangular wave, which is 0.45 here.

The total harmonic distortion rate of the currents, which represented by δ_{THDi} , can be expressed as

$$\delta_{\text{THDi}} = \frac{I_h}{I_1} \times 100\% = \sqrt{\frac{\sum_{n \geq 2}^{\infty} I_n^2}{I_1^2}} \times 100\%, \quad (23)$$

where I_1 represents the RMS value of fundamental current; I_h represents the RMS value of total harmonic currents.

With regard to the δ_{THDi} of zigzag 12-pulse transformer rectifier with current injection at DC side, calculating Eqs. (16), (22) and (23) by Matlab program can get that the average δ_{THDi} of grid-side in proposed rectifier is 1.24% theoretically, which is less than the 9.10%^[17] of conventional zigzag

12-pulse rectifier. So theoretically speaking, the active injection strategy can significantly reduce the δ_{THDi} on the grid side of the rectifying system.

The current hysteresis-band control method is adopted to generate the triangular waveform. This control method is easy to realize and it is closed-loop control with strong stability. Fig. 7 shows the control schematic diagram of the inverter.

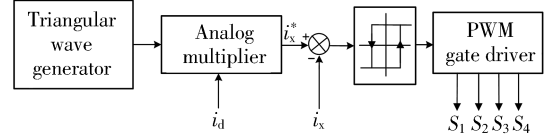


Fig. 7 Control block diagram of the inverter

The triangular wave generator produces a triangular wave with 6 times power frequency and amplitude of ± 0.45 . By comparing the reference current of multiplier with the injection current, the difference signal is connected to the hysteresis controller. After the hysteresis controller generates the driving signal to drive the single-phase inverter, the required 6 times power frequency injection currents which can change with the load current can be obtained.

5 Validation and analysis

In MATLAB/Simulink, the simulation model of the proposed low harmonic 12-pulse zigzag rectifying system is established. Fig. 8(a) and Fig. 8(b) show the simulation model of zigzag 12-pulse autotransformer and the auxiliary circuit, respectively.

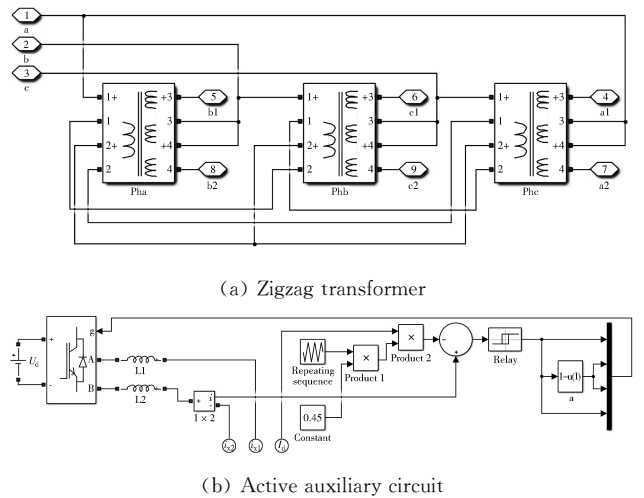


Fig. 8 Simulation model

Under the condition of the same power supply and same load, the proposed zigzag autotransformer rectifier is compared with the conventional zigzag

autotransformer rectifier. The simulation parameters are listed in Table 1.

Table 1 Parameters for simulation

Parameter	Description	Value
V_{LL} (V)	RMS value of input line voltage	380
$K_1 \cdot K_2$	Turn ratios of the windings	0.333 3+0.154 7
R_{load} (Ω)	DC load resistor	30
L_{load} (mH)	DC filter inductor	5
L_x (mH)	Inverter filter inductor	1.5
V_{DC} (V)	DC source of inverter	100
f_c (kHz)	Switching frequency of inverter	12
f (Hz)	AC supply frequency	50
B (A)	Current hysteresis band width	± 0.01

When the active auxiliary circuit is not working, the main simulation results of the rectifier are shown in Fig. 9.

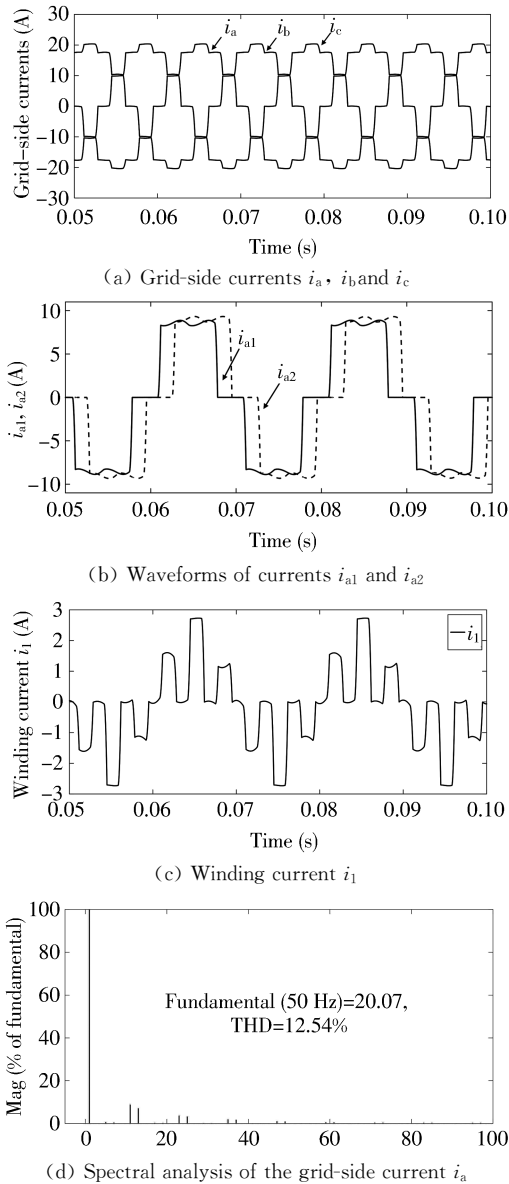


Fig. 9 Main simulation results of the rectifier when active auxiliary circuit is not working

Fig. 9(a) shows the current waveform on the grid side of the system without compensating currents. It can be seen that the waveform has been obviously distorted. Fig. 9(b) shows the waveforms current i_{a1} and i_{a2} . It can be verified from the figure that the phase difference of the two waveforms is 30° to achieve the effect of phase-shifting, indicating that the windings design of the zigzag autotransformer is correct. Fig. 9(c) shows the current i_1 in the winding of zigzag autotransformer. The waveforms of the winding currents i_2 and i_3 are consistent with i_1 but the phase difference is 120° . In the case of full load, Fig. 9(d) is the spectral analysis diagram of the three-phase grid-side current i_a , whose δ_{THD_i} is 12.54%. Obviously, conventional zigzag 12-pulse rectifier cannot meet the standards of IEEE-519^[18] and IEC 61000-3^[19] that the δ_{THD_i} shall be lower than 5%.

When the active auxiliary circuit is working, the waveform of the current i_{x1} in Fig. 10, which is generated by the auxiliary circuit in Fig. 8(b), is directly injected into the DC side of the proposed rectifier. The frequency of the current i_{x2} is the same as that of the current i_{x1} , both of which are triangular waves of 300 Hz with a phase difference of 30° .

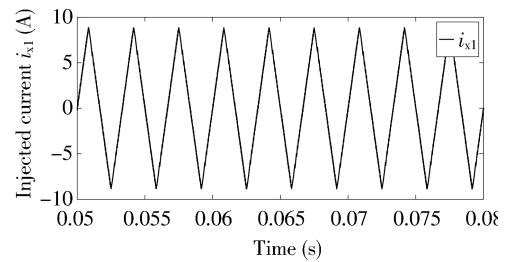


Fig. 10 Waveform of current i_{x1} injected into DC side

The injections of these two triangle waves make the waveforms of the output current i_{d1} and i_{d2} of the two DBRs triangular, as shown in Fig. 11(a). Although the waveforms of the output currents of the DBRs change after the current injection, the output currents' average values of the DC side are the same.

Accordingly, waveforms of input currents i_{a1} , i_{a2} and winding current i_1 of the DBRs have been improved, as shown in Fig. 11(b) and Fig. 11(c). As can be seen from Fig. 3, grid-side current i_a is synthesized by currents i_{a1} , i_{a2} and winding current i_1 , so its waveform should be close to the standard sine wave, as shown in Fig. 11(d).

According to the spectral analysis of the grid-side current i_a in Fig. 11(e), its δ_{THD_i} is 1.17%. Obviously, when the single-phase inverter is working, the grid-side δ_{THD_i} of the 12-pulse rectifying system is very small and can meet the harmonic

requirements of IEEE-519 and IEC 61000-3.

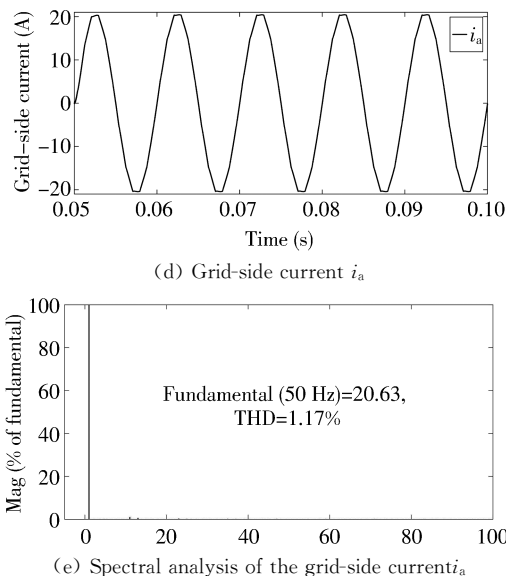
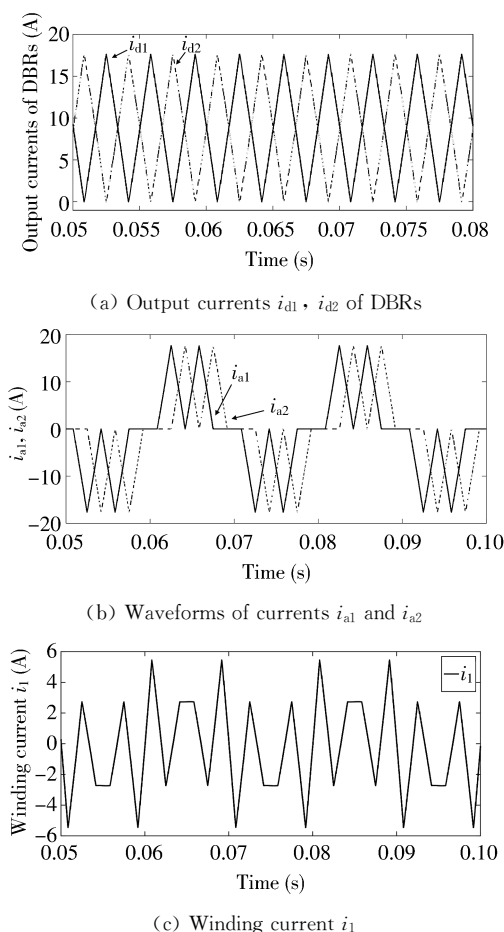


Fig. 11 Main simulation results of the rectifier when active auxiliary circuit is working

Under the condition of full load, Table 2 shows the harmonic parameters of the grid-side currents of the rectifying system after the injection of compensating currents. When no compensating currents are injected, the average grid-side δ_{THD_i} is 12.537% which is less than the theoretical value due to the influence of leakage inductance of transformer windings, but the δ_{THD_i} cannot meet the requirements^[18-19].

Table 2 Harmonic parameters comparison of grid-side currents with or without compensating currents

Compensating currents	Grid-side currents	δ_{THD_i} (%)	RMS of fundamental current (A)	Average of δ_{THD_i} (%)	Harmonic components (%)	
					11th	13th
Without	i_a	12.536	14.194	12.537	8.720	6.990
	i_b	12.537	14.195		8.720	6.990
	i_c	12.538	14.194		8.720	6.990
With	i_a	1.168	14.583	1.162	0.890	0.540
	i_b	1.156	14.582		0.900	0.540
	i_c	1.163	14.583		0.890	0.540

After the injection of compensating currents, the average δ_{THD_i} of three-phase grid-side currents is 1.162%. Obviously, conclusion can be drawn from Table 2 and Fig. 11(e) that the zigzag 12-pulse rectifier with active injection at DC side can not only reduce the average grid-side δ_{THD_i} , but also reduce the content of the 11th and the 13th harmonics.

After the compensation circuit is working and the selected load values are between 10% and 100% of the rated load, simulation is carried out to study the influence of various load on the grid-side currents. Fig. 12 shows the change trend. It can be clearly seen

that the harmonic content of the grid-side currents changes little with the load before and after current injection. Although the grid-side δ_{THD_i} increases when the rectifying system is under light load, as a whole, the harmonic content of the rectifying system after compensation can still meet the standards^[18-19].

According to Ref. [5], the equivalent capacity of the transformer can be calculated as

$$S_{eq} = 0.5 \times \sum V_{RMS} \times I_{RMS}, \quad (24)$$

where S_{eq} represents the equivalent capacity of the transformer; V_{RMS} represents the RMS value of

voltage at both ends of each winding of the transformer; I_{RMS} represents the RMS value of the current flowing through each winding of the transformer.

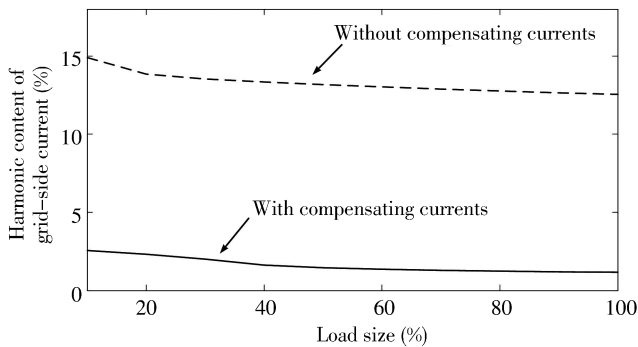


Fig. 12 Trend chart of grid-side currents harmonic content changing with load

The RMS value of currents fed to the windings of autotransformer, IPRs and single-phase inverter can be obtained by the simulation model. The equivalent capacity of the zigzag autotransformer, IPRs and inverter by computation is 23.35%, 2.11% and 2.21% of the output power of the load side respectively, so the total equivalent capacity of the magnetic elements in the whole system is 27.66%.

To demonstrate the correctness and applicability of constructing an active auxiliary circuit through a small capacity inverter, the δ_{THD_i} and equivalent capacity of two topologies, topology-A and topology-B, are compared in Table 3 under the condition of rated load, in which topology-A is the zigzag 12-pulse rectifier with boost converter^[20], topology-B is the proposed rectifier. By Table 3, the grid-side δ_{THD_i} of topology-B is 1.17%, which is less than 2.64% of that of topology-A. In terms of the equivalent capacity of this two rectifiers, due to the different harmonic suppression methods on the DC side, the winding currents of the autotransformer, IPRs and auxiliary circuit also vary. Table 3 shows that the equivalent capacity of topology-A is 3.54% higher than that of topology-B, indicating that topology-B gets higher power density. Therefore, the topology-B has better performance in the aspect of the effect of the rectifying system on the grid-side currents and the equivalent capacity of whole system.

Table 3 Comparison of parameters for different topologies

	δ_{THD_i} (%)	S_{Auto} (%)	S_{IPR} (%)	S_{CIC} (%)	S_{eq} (%)
A	2.64	25.54	3.40	2.27	31.21
B	1.17	23.35	2.11	2.21	27.67

6 Conclusions

A zigzag 12-pulse rectifier by active injection at DC side has been proposed. The calculation method of the winding configuration parameters of zigzag phase-shifting autotransformer is given. When the grid-side currents are sinusoidal, the current waveform of active injection compensation is analyzed. At last, the rectifying system model is built and the theoretical analysis is confirmed by simulation. The conclusions can be draw as follows:

1) When the output currents of the auxiliary circuit are triangular and their frequency is 6 times grid frequency, the grid-side δ_{THD_i} is about 1.17%. Hence the current harmonics are notably suppressed.

2) When the load is changed, the current hysteresis-band control method used by the multi-pulse rectifier can adjust the output compensating currents, which can restrain the increase of the harmonics content of the grid-side current.

3) After using zigzag autotransformer as phase-shifting transformer and using small capacity inverter to generate compensating currents, the system equivalent capacity is only about 27% of the load power, which can reduce the volume and improve the power density of rectifying system.

References

- [1] Shahbaz K, Zhang X B, Muhammad S, et al. Comparative analysis of 18-pulse autotransformer rectifier unit topologies with intrinsic harmonic current cancellation. *Energies*, 2018, 11(6): 1347.
- [2] Meng F, Wei Y, Yang S, et al. Active harmonic reduction for 12-pulse diode bridge rectifier at DC side with two-stage auxiliary circuit. *IEEE Transactions on Industrial Informatics*, 2017, 11(1): 64-73.
- [3] Fangang M, Shiyan Y, Wei Y. Overview of multi-pulse rectifier technique. *Electric Power Automation Equipment*, 2012, 32(2): 9-22.
- [4] Chen J L, Li Y H, Jiang X J, et al. Control methods of hybrid active power filter reduced its converter rating. *Transactions of China Electrotechnical Society*, 2009, 24(4): 214-218.
- [5] Paice D. *Power electronics converter harmonics: multi-pulse methods for clean power*. Wiley: IEEE Press, 1996.
- [6] Araujo-Vargas I, Forsyth A J, Chivite-Zabalza F J. Capacitor voltage-balancing techniques for a multipulse rectifier with active injection. *IEEE Transactions on Industry Applications*, 2011, 47(1): 185-198.
- [7] Hamadi A, Rahmani S, Al-Haddad K. Digital control of

- a shunt hybrid power filter adopting a nonlinear control approach. *IEEE Transactions on Industrial Informatics*, 2013, 9(4): 2092-2104.
- [8] Rodriguez J R, Pontt J, Silva C, et al. Large current rectifiers: state of the art and future trends. *IEEE Transactions on Industrial Electronics*, 2005, 52(3): 738-746.
- [9] Meng F G, Yang W, Yang S. Active harmonic suppression of paralleled 12-pulse rectifier at DC side. *Science in China Series E: Technological Sciences*, 2011, 54(12): 3320-3331.
- [10] Biela J, Hassler D, Schönberger J, et al. Closed-loop sinusoidal input-current shaping of 12-pulse autotransformer rectifier unit with impressed output voltage. *IEEE Transactions on Power Electronics*, 2011, 26(1): 249-259.
- [11] Chen X Q, Zhao S W, Wang Y. Simulation of a kind of active harmonic reduction 18-pulse rectifier. *Journal of Measurement Science and Instrumentation*, 2018, 9(2): 160-168.
- [12] Young C M, Wu S F, Yeh W S, et al. A DC-side current injection method for improving AC line condition applied in the 18-pulse converter system. *IEEE Transactions on Power Electronics*, 2014, 29(1): 99-109.
- [13] Liu K, Cao W, You J, et al. Improved parallel operation for multi-modular shunt APF using dual harmonic compensation loop. In: *Proceedings of 2016 IEEE 8th International Power Electronics and Motion Control Conference*, Hefei, China, 2016.
- [14] Meng F G, Liu P Y, Sun Z N, et al. Active harmonic elimination of a large current rectifier based on star-connected autotransformer. In: *Proceedings of 2016 IEEE 8th International Power Electronics and Motion Control Conference*, Hefei, China, 2016.
- [15] Choi S, Jang M. Analysis and control of a single-phase inverter zigzag-transformer hybrid neutral-current suppressor in three-phase four-wire systems. *IEEE Transactions on Industrial Electronics*, 2007, 54(4): 2201-2208.
- [16] Singh B, Bhuvaneswari G, Garg V, et al. Pulse multiplication in AC-DC converters for harmonic mitigation in vector-controlled induction motor drives. *IEEE Transactions on Energy Conversion*, 2006, 21(2): 342-352.
- [17] Singh B, Gairola S. Pulse multiplication in autotransformer based AC-DC converters using A zigzag connection. *Journal of Power Electronics*, 2007, 7(3): 191-202.
- [18] IEEE Standard 519-1992. *IEEE guide for harmonic control and reactive compensation of static power converters*. New York: Institute of Electrical and Electronic Engineers (IEEE), 1992.
- [19] International Electro-technical Commission Standard 61000-3-2. *Limits for harmonic current emissions*. Geneva: International Electrotechnical Commission (IEC), 2004.
- [20] Vidyasagar V S, Kalpana R, Singh B, et al. Improvement in Harmonic Reduction of Zigzag Autoconnected Transformer Based 12-pulse Diode Bridge Rectifier by Current Injection at DC Side. *IEEE Transactions on Industry Applications*, 2017, 53(6): 5634-5644.

一种基于直流侧有源注入的 12 脉波 之字形自耦变压整流器

刘炯德¹, 陈小强^{1,2}, 王英¹, 陈涛¹

(1. 兰州交通大学 自动化与电气工程学院, 甘肃 兰州 730070;

2. 兰州交通大学 光电技术与智能控制教育部重点实验室, 甘肃 兰州 730070)

摘要: 为提高多脉波整流器的谐波抑制能力, 提出了一种基于直流侧有源补偿策略的之字形自耦变压整流器。通过控制小容量电流逆变器产生补偿电流, 并将补偿电流直接注入到系统的直流侧使整流器输入电流近似为正弦波。使用之字形自耦变压器作为移相变压器以阻断零序电流成分, 降低整流系统的等效容量。研究网侧电流谐波畸变率随负载的变化规律表明, 在各种负载条件下, 补偿后的整流系统谐波含量显著降低。所提出的有源注入整流系统的网侧电流谐波含量仅为 1.17%, 且具有较低的等效容量。

关键词: 多脉波整流器; 有源补偿; 之字形自耦变压器; 等效容量

引用格式: LIU Jiongde, CHEN Xiaoqiang, WANG Ying, et al. A low harmonic 12-pulse rectifier based on zigzag autotransformer by current injection at DC side. *Journal of Measurement Science and Instrumentation*, 2021, 12(3): 347-355. DOI: 10.3969/j.issn.1674-8042.2021.03.013